

A Direct Second-Order Method for Solving Two-Player Zero-Sum Games

David Yang* Yuan Gao† Tianyi Lin‡ Christian Kroer‡

Abstract

We introduce, to our knowledge, the first direct second-order method for computing Nash equilibria in two-player zero-sum games. To do so, we construct a Douglas-Rachford-style splitting formulation, which we then solve with a semi-smooth Newton (SSN) method. We show that our algorithm enjoys local superlinear convergence. In order to augment the fast local behavior of our SSN method with global efficiency guarantees, we develop a hybrid method that combines our SSN method with the state-of-the-art first-order method for game solving, Predictive Regret Matching⁺ (PRM⁺). Our hybrid algorithm leverages the global progress provided by PRM⁺, while achieving a local superlinear convergence rate once it switches to SSN near a Nash equilibrium. Numerical experiments on matrix games demonstrate order-of-magnitude speedups over PRM⁺ for high-precision solutions.

*Columbia University. Corresponding author, dy2507@columbia.edu.

†Microsoft.

‡Columbia University.

1 Introduction to Bilinear Saddle Point Problem

The Nash equilibrium is arguably the most foundational solution concept of game theory, representing a strategy profile in which no player can unilaterally deviate to improve their outcome. Approximating Nash equilibria of large-scale game models is the foundation of many human and superhuman-level AIs for games such as poker [Bowling et al., 2015, Brown and Sandholm, 2018, 2019], Stratego [Perolat et al., 2022], and Diplomacy [FAIR et al., 2022].

In the two-player zero-sum game setting, one player’s gain is the other player’s loss, so the game is completely described by a single payoff (utility) matrix $A \in \mathbb{R}^{n \times m}$, where entry a_{ij} specifies the utility of the column player (and the negative utility of the row player) when the actions i and j are played. A (mixed-strategy) Nash equilibrium is then a pair of probability distributions (x^*, y^*) over the rows and columns of A , such that x^* and y^* minimize and maximize their expected payoffs, respectively, given the strategy of the other player.

By von Neumann’s minimax theorem, finding a Nash equilibrium in a two-player zero-sum game can be formulated as solving the bilinear saddle point problem (BLSP)

$$\min_{x \in X} \max_{y \in Y} x^\top A y \tag{1.1}$$

where $A \in \mathbb{R}^{n \times m}$ is the payoff matrix and $X \subseteq \mathbb{R}^n$, $Y \subseteq \mathbb{R}^m$ are convex, compact strategy sets for the min and max players.

In both normal-form and extensive-form games, X and Y are polytopes, and so the optimization problem in Equation (1.1) can be solved exactly by linear programming [Von Stengel, 1996]. While this approach works in principle, it is impractical for large-scale games; even with state-of-the-art commercial solvers, the LP reformulation inflates the problem size and removes exploitable structures in the payoff and constraint matrices, making exact solutions computationally prohibitive. Instead, first-order methods (FOMs) and regret minimization approaches have been widely used for large-scale game solving, where they have been highly successful in scaling to and solving large games arising from real-world applications. FOMs such as the *Extragradient Method* [Korpelevich, 1976] and *Mirror Prox* [Nemirovski, 2004] converge to a Nash equilibrium at a rate of $O(1/T)$, where T is the number of iterations. Regret minimization approaches include *Regret Matching*⁺ (RM⁺) and its predictive variant *Predictive Regret Matching*⁺ (PRM⁺) [Zinkevich et al., 2007]; these approaches use self-play to iteratively update each player’s strategy proportional to their positive cumulative regrets, and converge to a Nash equilibrium at a rate of $O(1/\sqrt{T})$, though their empirical performance is often much stronger. In fact, *Counterfactual Regret Minimization*⁺ (CFR⁺) [Tammelin, 2014] and its predictive variant PCFR⁺ [Farina et al., 2021], which extend the RM⁺ framework from normal-form to extensive-form games, are some of the fastest game-solving algorithms numerically, and CFR⁺ served as the foundation for recent breakthroughs in superhuman poker AIs [Bowling et al., 2015, Brown and Sandholm, 2018, 2019].

While FOMs serve as the standard for computing approximate Nash equilibrium in two-player zero-sum games, their sublinear convergence guarantees make high-precision solutions expensive to compute. In convex minimization, high-precision solutions can be computed with second-order methods, which exploit curvature information for rapid local convergence. In two-player zero-sum game solving, however, there are no known “direct” methods for computing Nash equilibria using second-order methods. Classical second-order methods in optimization, such as interior-point

algorithms, exploit curvature information through barrier formulations to achieve polynomial-time complexity for constrained problems. These methods can be applied by converting the BLSP into a linear program and applying the interior-point methods to that formulation. However, this throws away much of the structure of the BLSP and forces the use of generic methodology. Recently, there have been advances in applying second-order methods directly to saddle point problems, such as the J -symmetric quasi-Newton framework of [Asl et al. \[2024\]](#), but these advances are restricted to the unconstrained setting. In contrast, our method offers a direct means of incorporating curvature information into bilinear saddle point problems, without resorting to barrier reformulations or unconstrained analogues, while simultaneously leveraging the strengths of the state-of-the-art FOMs in game solving. As a first step to leverage the power of the curvature information inherent in the strategy spaces, we present a hybrid method combining a state-of-the-art FOM with a semi-smooth Newton method applied to an operator stemming from the Douglas-Rachford splitting algorithm (DRS). Our main results are as follows.

Principled Use of Curvature Information. To the best of our knowledge, we develop the first direct second-order method for solving bilinear saddle point problems, based on a Douglas–Rachford splitting formulation solved via a regularized semi-smooth Newton method. In contrast to other saddle point residual operators, our residual operator derived from DRS is monotone and piecewise affine, making it particularly well-suited for SSN methods. We establish that the regularized semi-smooth Newton method applied to our residual operator achieves local quadratic convergence. Our analysis replaces the classical BD-regularity assumption [[Facchinei and Pang, 2003](#)] with a local error bound condition and a stability property implied by monotonicity and Lipschitz continuity. In doing so, we extend prior metric-subregularity results for matrix games [[Tseng, 1995](#), [Gilpin et al., 2012](#), [Wei et al., 2021](#)] to our residual operator using tools from convex analysis.

First and Second-order Hybrid Method. While our second-order method has local superlinear convergence, it may be slow initially. To ameliorate this fact, we develop a principled approach for switching between iterates generated by a first-order method, which generally lie in the feasible set, and iterates for our SSN method, which generally move outside the feasible set. By systematically leveraging the progress of PRM^+ to warm-start our regularized semi-smooth Newton method, our approach provides the first framework combining first-order progress with second-order guarantees, ensuring efficient global progress together with local superlinear convergence as our method transitions to SSN steps. A key component of our design is a lifting framework that allows for an effective transition: given a strong FOM iterate, the corresponding lifted SSN iterate has a small residual norm, placing it squarely within the regime of local superlinear convergence.

Numerical Experiments. We conduct extensive numerical experiments on a diverse set of matrix games. For finding low-precision regimes, our hybrid method can be slower than pure FOMs due to a preprocessing inversion step and the overhead of solving Newton systems. However, once the SSN iterates enter a neighborhood of a Nash equilibrium in the lifted space, our hybrid method effectively exploits second-order information, leading to significant speedup over state-of-the-art FOMs. The results validate both the theoretical guarantees and the practical efficiency of our approach for high-precision equilibrium computation.

2 Preliminaries and Technical Background

We provide the formal definitions for two-player zero-sum games considered in this paper, and the schemes of operator splitting methods and semi-smooth Newton methods.

2.1 Two-Player Zero-Sum Games

We denote by $\mathcal{S} = \Delta^n \times \Delta^m$ the set of feasible strategy profiles, where Δ^n and Δ^m are the simplices representing the mixed strategies of the two players in an $n \times m$ zero-sum matrix game with payoff matrix A . A generic strategy profile will be written as $z := (x, y)$, with $x \in \Delta^n$ representing the minimizer's strategy and $y \in \Delta^m$ the maximizer's strategy. Within this framework, the duality gap serves as a natural measure of how far a strategy profile is from the set of Nash equilibria: it quantifies the incentive for either player to unilaterally deviate from their current strategies.

Definition 1. For a strategy profile $\hat{z} = (\hat{x}, \hat{y})$, the duality gap is defined as

$$\text{gap}(\hat{z}) = \max_{y \in \Delta^m} \hat{x}^\top A y - \min_{x \in \Delta^n} x^\top A \hat{y}. \quad (2.1)$$

By definition, \hat{z} is a Nash equilibrium if and only if $\text{gap}(\hat{z}) = 0$.

The maximizer evaluates the highest payoff achievable by deviating from \hat{y} , while the minimizer evaluates the lowest payoff achievable by deviating from \hat{x} , demonstrating that $\text{gap}(\hat{z}) \geq 0$ always holds. In practice, iterative algorithms for computing Nash equilibria seldom converge exactly to an equilibrium, but rather produce approximate solutions. This motivates the notion of an ϵ -Nash equilibrium, where the incentives to deviate are bounded by a small tolerance $\epsilon > 0$.

Definition 2. A strategy profile $\hat{z} = (\hat{x}, \hat{y})$ is an ϵ -Nash equilibrium if the following condition holds:

$$\max_{y \in \Delta^m} \hat{x}^\top A y - \epsilon \leq \hat{x}^\top A \hat{y} \leq \min_{x \in \Delta^n} x^\top A \hat{y} + \epsilon.$$

Remark 1. The concept of an ϵ -Nash equilibrium can be equivalently expressed in terms of the duality gap [Orabona, 2019]. Specifically, if \hat{z} is an ϵ -Nash equilibrium, then its duality gap satisfies $\text{gap}(\hat{z}) \leq 2\epsilon$. Conversely, if a strategy profile \hat{z} achieves a duality gap below ϵ , then \hat{z} itself constitutes an ϵ -Nash equilibrium. This tight connection establishes the duality gap as a natural and widely used performance metric for analyzing iterative algorithms.

2.2 Operator Splitting Methods

As an alternative to the duality gap, Nash equilibria can also be characterized through residual operators. A natural choice is the classical saddle-point normal map $z \mapsto z - \Pi_{\mathcal{S}} \left(z - \eta \begin{bmatrix} 0 & A \\ -A^\top & 0 \end{bmatrix} z \right)$, but this map is not monotone in the two-player zero-sum game setting and therefore lacks a desired structural property for SSN methods. Instead, we base our construction on the optimality condition for two-player zero-sum games: a strategy profile $\hat{z} = (\hat{x}, \hat{y}) \in \mathcal{S}$ is a Nash equilibrium if and only if $0 \in F(\hat{z}) + N_{\mathcal{S}}(\hat{z})$ where

$$F(\hat{z}) = \begin{bmatrix} 0 & A \\ -A^\top & 0 \end{bmatrix} \hat{z}, \quad N_{\mathcal{S}}(\hat{z}) = \{v \mid v^\top (z - \hat{z}) \leq 0 \quad \forall z \in \mathcal{S}\}.$$

Thus, finding a Nash equilibrium reduces to finding a root of the sum of two structured operators. From standard convex analysis, both $F(\cdot)$ and $N_{\mathcal{S}}(\cdot)$ are maximally monotone, which guarantees that their resolvents $J_F^\gamma(\cdot) = (I + \gamma F)^{-1}(\cdot)$ and $J_{N_{\mathcal{S}}}^\gamma = (I + \gamma N_{\mathcal{S}})^{-1}(\cdot)$ are single-valued and firmly nonexpansive. This fact underpins the use of operator-splitting methods in solving two-player zero-sum games; for an overview of such methods, see the monographs [Rockafellar and Wets \[1998\]](#), [Bauschke and Combettes \[2017\]](#), [Ryu and Yin \[2022\]](#).

In particular, we focus on the Douglas-Rachford splitting (DRS) method [[Lions and Mercier, 1979](#), [Eckstein and Bertsekas, 1992](#)], which applies to sums of two maximal monotone operators. With step size $\gamma > 0$, the DRS operator applied to our setting is given by

$$T_{\text{DRS}}^\gamma = \text{Id} - J_{N_{\mathcal{S}}}^\gamma + J_F^\gamma \circ (2J_{N_{\mathcal{S}}}^\gamma - \text{Id}), \quad (2.2)$$

where Id denotes the identity operator and \circ represents composition. Because $F(\cdot)$ is linear and $N_{\mathcal{S}}(\cdot)$ is a normal cone operator, their resolvents simplify to

$$J_F^\gamma(z) = \begin{bmatrix} I & \gamma A \\ -\gamma A^\top & I \end{bmatrix}^{-1} z, \quad J_{N_{\mathcal{S}}}^\gamma(z) = \Pi_{\mathcal{S}}(z).$$

Thus, J_F^γ is a linear operator and $J_{N_{\mathcal{S}}}^\gamma$ is simply the projection onto \mathcal{S} . As a consequence, one DRS iteration takes the following form of

$$z_{k+1} = T_{\text{DRS}}^\gamma(z_k) = z_k - \Pi_{\mathcal{S}}(z_k) + \begin{bmatrix} I & \gamma A \\ -\gamma A^\top & I \end{bmatrix}^{-1} (2\Pi_{\mathcal{S}}(z_k) - z_k). \quad (2.3)$$

We define the residual operator $R_{\text{DRS}}^\gamma := \text{Id} - T_{\text{DRS}}^\gamma$, noting that $R_{\text{DRS}}^\gamma(\hat{z}) = 0$ implies $\Pi_{\mathcal{S}}(\hat{z})$ is a Nash equilibrium (see Section 3.1). The following lemma summarizes one of its key properties.

Lemma 1. *The operator $R_{\text{DRS}}^\gamma(\cdot)$ is*

- (i) *monotone:* $(z_1 - z_2)^\top (R_{\text{DRS}}^\gamma(z_1) - R_{\text{DRS}}^\gamma(z_2)) \geq 0$
- (ii) *1-Lipschitz:* $\|R_{\text{DRS}}^\gamma(z_1) - R_{\text{DRS}}^\gamma(z_2)\| \leq \|z_1 - z_2\|$

for all z_1, z_2 .

Our approach is to solve the root-finding problem for this residual operator using semi-smooth Newton (SSN) methods [[Qi and Sun, 1993](#), [Pang and Qi, 1993](#), [Mart'inez and Qi, 1995](#)]. This shares a similar spirit with prior SSN applications in composite convex optimization [[Xiao et al., 2018](#)] and kernel-based optimal transport [[Lin et al., 2024](#)].

However, the unique structure of two-player zero-sum games requires new algorithmic strategies, including nontrivial switching between SSN and PRM⁺, making the practical implementation considerably more delicate.

2.3 Semi-smooth Newton Methods

Semi-smooth Newton (SSN) methods generalize the classical Newton method to nonsmooth equations by replacing the Jacobian with a generalized Jacobian. Since $R_{\text{DRS}}^\gamma(\cdot)$ is Lipschitz continuous, Rademacher's theorem implies that it is differentiable almost everywhere. This motivates the use of the notion of a generalized Jacobian [[Clarke, 1990](#)].

Definition 3. Let F be a Lipschitz mapping and D_F the set of differentiable points of F . The B -subdifferential at z is $\partial_B F(z) = \{\lim_{k \rightarrow +\infty} \nabla F(z^k) \mid z^k \in D_F, z^k \rightarrow z\}$ and the generalized Jacobian is defined as $\partial F(z) = \text{conv}(\partial_B F(z))$, where conv denotes the convex hull.

A second key notion is semi-smoothness, introduced by [Mifflin \[1977\]](#) for real-valued functions and extended to vector-valued mappings by [Qi and Sun \[1993\]](#).

Definition 4. Let F be a Lipschitz mapping. Then F is (strongly) semi-smooth at z if (i) F is directionally differentiable at z , and (ii) for any $G \in \partial F(z + \Delta z)$, as $\Delta z \rightarrow 0$,

$$\begin{aligned} \text{(semismooth)} \quad & \frac{\|F(z+\Delta z) - F(z) - G\Delta z\|}{\|\Delta z\|} \rightarrow 0, \\ \text{(strongly semismooth)} \quad & \frac{\|F(z+\Delta z) - F(z) - G\Delta z\|}{\|\Delta z\|^2} \leq C \end{aligned}$$

for some constant $C > 0$.

The following lemma shows that $R_{\text{DRS}}^\gamma(\cdot)$ is strongly semi-smooth and guarantees that the SSN method is suitable to solve $R_{\text{DRS}}^\gamma(z) = 0$.

Lemma 2. The operator $R_{\text{DRS}}^\gamma(\cdot)$ is strongly semi-smooth.

This property justifies the use of SSN to solve $R_{\text{DRS}}^\gamma(z) = 0$. In particular, the regularized SSN method proceeds as follows: given z_k , compute $z_{k+1} = z_k + \Delta z_k$, where Δz_k solves

$$(G_k + \mu_k I)\Delta z_k = -r_k, \tag{2.4}$$

with $G_k \in \partial R_{\text{DRS}}^\gamma(z_k)$, $r_k = R_{\text{DRS}}^\gamma(z_k)$, and I the identity matrix. The regularization parameter is chosen adaptively as $\mu_k = \theta_k |r_k|$ for $\theta_k > 0$. This stabilizes the method in practice: as $r_k \rightarrow 0$, the algorithm gradually exploits curvature information from G_k while maintaining invertibility of $G_k + \mu_k I$.

If R is continuously differentiable and $\theta_k = 0$, this reduces to the Newton method, which exhibits local quadratic convergence. Although regularized SSN methods may diverge in general [\[Kummer, 1988\]](#), local superlinear convergence is guaranteed under strong semi-smoothness and local error bound conditions [\[Zhou and Toh, 2005\]](#).

3 Main Results

In this section, we first establish a formal connection between Nash equilibria and lifted fixed points, which serves as the theoretical foundation of our approach. Second, building on this insight, we introduce a new game-solving algorithm that integrates PRM⁺ with a regularized semi-smooth Newton method. Finally, we provide a convergence analysis of the resulting procedure.

3.1 Linking Nash Equilibria to Lifted Fixed Points

While Nash equilibria are not themselves fixed points of T_{DRS}^γ , they can be linked through a simple lifting, as the following theorem shows.

Theorem 1. *The following relationships between fixed points of T_{DRS}^γ and Nash equilibria hold:*

(i) *If $z \in \mathbb{R}^{m+n}$ is a fixed point of T_{DRS}^γ , then $\hat{z} = \Pi_{\mathcal{S}}(z)$ is a Nash equilibrium.*

(ii) *If $\hat{z} \in \mathcal{S}$ is a Nash equilibrium, then $z = \hat{z} - \gamma F(\hat{z})$ is a fixed point of T_{DRS}^γ .*

Remark 2. *A Nash equilibrium is not necessarily a fixed point of T_{DRS}^γ . Indeed, since $\Pi_{\mathcal{S}}(\hat{z}) = \hat{z}$, we have*

$$T_{\text{DRS}}^\gamma(\hat{z}) = \hat{z} - \Pi_{\mathcal{S}}(\hat{z}) + \begin{bmatrix} I & \gamma A \\ -\gamma A^\top & I \end{bmatrix}^{-1} (2\Pi_{\mathcal{S}}(\hat{z}) - \hat{z}) = \begin{bmatrix} I & \gamma A \\ -\gamma A^\top & I \end{bmatrix}^{-1} \hat{z}.$$

Thus, \hat{z} is a fixed point of T_{DRS}^γ if and only if $A = 0$, which does not hold in general. The role of the lifted point $z = \hat{z} - \gamma F(\hat{z})$ is to displace \hat{z} along its normal cone direction, which ensures the fixed-point relation.

To implement the SSN method, we require an efficient way to obtain one element in $\partial R_{\text{DRS}}^\gamma$. By definition, we have

$$R_{\text{DRS}}^\gamma = J_{N_{\mathcal{S}}}^\gamma - J_F^\gamma \circ (2J_{N_{\mathcal{S}}}^\gamma - \text{Id}),$$

where

$$J_F^\gamma(z) = \begin{bmatrix} I & \gamma A \\ -\gamma A^\top & I \end{bmatrix}^{-1} z, \quad J_{N_{\mathcal{S}}}^\gamma(z) = \Pi_{\mathcal{S}}(z).$$

The generalized Jacobian of $R_{\text{DRS}}^\gamma(\cdot)$ at z is given by

$$\partial R_{\text{DRS}}^\gamma(z) = \partial J_{N_{\mathcal{S}}}^\gamma(z) - (\partial J_F^\gamma) \circ (2\partial J_{N_{\mathcal{S}}}^\gamma(z) - z) \cdot (2\partial J_{N_{\mathcal{S}}}^\gamma(z) - I),$$

where

$$\partial J_F^\gamma(z) = \begin{bmatrix} I & \gamma A \\ -\gamma A^\top & I \end{bmatrix}^{-1}, \quad \partial J_{N_{\mathcal{S}}}^\gamma = \partial \Pi_{\mathcal{S}}(z) = \left\{ \begin{bmatrix} G_x & 0 \\ 0 & G_y \end{bmatrix} : G_x \in \partial \Pi_{\Delta^n}(x), G_y \in \partial \Pi_{\Delta^m}(y) \right\}.$$

Thus, finding an element in $\partial R_{\text{DRS}}^\gamma$ reduces to finding an element of the generalized Jacobian of the simplex projection operator.

Theorem 2. *Let $p \in \mathbb{R}^d$ and let $x = \Pi_{\Delta^d}(p)$ denote the projection of p onto the simplex Δ^d . Define the active set $\mathcal{A} := \{i \in [d] : x_i > 0\}$. Then*

$$G = \text{diag}(a) - \frac{1}{\|a\|_1} a a^\top,$$

where $a \in \mathbb{R}^d$ is the indicator vector of the active set \mathcal{A} , satisfies $G \in \partial \Pi_{\Delta^d}(p)$.

Putting these pieces together yields

$$\begin{bmatrix} G_x & 0 \\ 0 & G_y \end{bmatrix} - \begin{bmatrix} I & \gamma A \\ -\gamma A^\top & I \end{bmatrix}^{-1} \left(2 \begin{bmatrix} G_x & 0 \\ 0 & G_y \end{bmatrix} - I \right) \in \partial R_{\text{DRS}}^\gamma(z). \quad (3.1)$$

Theorem 1 establishes that projecting a fixed point of T_{DRS}^γ onto \mathcal{S} yields a Nash equilibrium, and conversely, every Nash equilibrium induces a lifted fixed point. These results demonstrate a one-to-one correspondence between exact fixed points and exact Nash equilibria.

In practice, however, algorithms rarely reach exact solutions; instead, they operate with approximate fixed points and ϵ -Nash equilibria. We therefore extend this correspondence to the approximate setting. In particular, we show how the residual norm of $R_{\text{DRS}}^\gamma(\cdot)$ can be related to the duality gap. This link guarantees that progress made by a first-order method (which decreases the duality gap) translates into progress for the semi-smooth Newton method (which works to decrease the residual norm), and vice versa. As such, the connection enables a principled transition between the two regimes within our proposed algorithmic framework.

To formalize this relationship, we require the following condition measure of the payoff matrix A , which is used to control the Euclidean distance to the set of equilibria in terms of the duality gap. Being able to relate the duality gap to the iterate distance serves as an essential tool in our analysis.

For the following discussion, we let Z^* denote the set of zeros of $R_{\text{DRS}}^\gamma(\cdot)$ and let \hat{Z}^* denote the set of Nash equilibria of \mathcal{S} .

Definition 5 (Condition Measure [Gilpin et al., 2012]). *The condition measure of a matrix A , denoted $\delta(A)$, is defined as*

$$\delta(A) = \sup \left\{ \delta : \text{dist}(\hat{z}, \hat{Z}^*) \leq \frac{\text{gap}(\hat{z})}{\delta} \text{ for all } \hat{z} \in \mathcal{S} \right\}.$$

Remark 3. *In addition, Gilpin et al. [2012, Lemma 4] guarantees that there exists $\delta > 0$ such that*

$$\text{dist}(\hat{z}, \hat{Z}^*) \leq \frac{\text{gap}(\hat{z})}{\delta} \tag{3.2}$$

for all $\hat{z} \in \mathcal{S}$. Thus, we have $\delta(A) < +\infty$ for any two-player zero-sum game.

Theorem 3. *Let $\hat{z} \in \mathcal{S}$. The following relationships hold:*

(i) *If $\|R_{\text{DRS}}^\gamma(z)\| \geq \tau \text{dist}(z, Z^*)$ for some constant $\tau > 0$, we have*

$$\text{gap}(\Pi_{\mathcal{S}}(z)) \leq \frac{\sqrt{2}\|A\| \cdot \|R_{\text{DRS}}^\gamma(z)\|}{\tau}.$$

(ii) *For the lifted point $z = \hat{z} - \gamma R_{\text{DRS}}^\gamma(\hat{z})$, we have*

$$\|R_{\text{DRS}}^\gamma(z)\| \leq \frac{(1 + \gamma\|A\|)\text{gap}(\hat{z})}{\delta(A)}.$$

3.2 Algorithmic Framework

We now outline the general framework of our algorithm and refer the reader to [Section B](#) for additional details.

The core idea is to warm-start our Douglas-Rachford-based regularized SSN method (DRSSN) using iterates generated by a phase of exclusively PRM⁺ steps. The PRM⁺ phase reduces the duality gap to bring iterates sufficiently close to a Nash equilibrium, thereby avoiding the instability that can arise when DRSSN is initialized by lifting an iterate arbitrarily far from a Nash equilibrium,

Algorithm 1 Hybrid SSN method

- 1: **Input:** $p_0 = z_0 \in \Delta^n \times \Delta^m$, $\theta_0 > 0$, $\gamma > 0$
 - 2: Calculate resolvent for DRSSN method
 - 3: **for** $k = 0, 1, \dots$ **do**
 - 4: Update $p_{k+1} = p_k$ using one-step of PRM⁺.
 - 5: **if** ready to update θ_k **then**
 - 6: Update θ_k adaptively.
 - 7: **if** ready to switch to DRSSN method **then**
 - 8: Set $z_k = p_k - \gamma F(p_k)$.
 - 9: Run DRSSN(z_k, θ_k).
-

Algorithm 2 DRSSN(z, λ)

- 1: **Input:** $z_0 = z \in \mathbb{R}^{n+m}$, $\lambda_0 = \lambda > 0$, $\ell = 1.5$
 - 2: **for** k in $0, 1, \dots$, **do**
 - 3: **while** $\lambda_k \leq 10^9$ **do**
 - 4: Select $G_k \in \partial R_{\text{DRS}}^\gamma(z_k)$.
 - 5: Use G_k and solve the linear system in [Equation \(2.4\)](#) for Δz_k .
 - 6: Define $z' := z_k + \Delta z_k$.
 - 7: **if** $\|R_{\text{DRS}}^\gamma(z')\| < \|R_{\text{DRS}}^\gamma(z_k)\|$ **then**
 - 8: Set $z_{k+1} = z'$.
 - 9: Update $\lambda_{k+1} = \lambda_k \cdot \ell$.
 - 10: **break**
 - 11: **else**
 - 12: Update $\lambda_{k+1} = \lambda_k / \ell$.
 - 13: Update λ_{k+1} using the adaptive scheme.
 - 14: **if** $\text{gap}(\Pi_S(z_{k+1}))$ is under desired gap **then**
 - 15: **return** $\Pi_S(z_{k+1})$.
-

starting a regime where curvature information is not yet informative. Moreover, the steps in the PRM⁺ phase can be used to update the damping parameter for DRSSN. After the duality gap drops below a prescribed threshold, our algorithm makes a one-time switch from PRM⁺ to DRSSN, after which only Newton steps are taken. This design ensures global efficiency from the first-order phase and rapid local convergence from the second-order phase.

The DRSSN subroutine implements our regularized semi-smooth Newton method. Each iteration involves solving a linear system to compute the Newton step Δz_k , followed by a damping parameter update that depends on changes in the residual norm $\|R_{\text{DRS}}^\gamma\|$. While the duality gap is the standard measure of proximity to a Nash equilibrium and is natural for first-order methods that remain within the feasible strategy spaces, it is less effective for guiding second-order methods. In particular, the SSN iterates may leave the feasible region, and relying solely on the projected duality gap may fail to capture true progress. Instead, effective performance of our SSN method hinges on proper tuning of the damping parameter to control the residual norm, which in turn governs its convergence.

This distinction is crucial in our hybrid algorithm. The first-order phase reduces the duality gap to a chosen threshold, ensuring a stable lifted iterate for the second-order phase. In particular, if

the duality gap of the PRM⁺ iterates is sufficiently small, then by [Theorem 3](#), the residual norm of the corresponding lifted point is appropriately bounded, ensuring that it lies within the regime where our SSN theory guarantees local superlinear convergence. The second-order phase advances through Newton steps while adaptively adjusting the damping parameter based on the residual norm, thereby exploiting curvature information to achieve accelerated convergence. To this end, our SSN method employs two damping-update strategies: (i) a line-search regime, which adjusts the parameter according to whether the residual norm decreases, thus ensuring consistent global progress when iterates are far from equilibrium; and (ii) an adaptive regime, inspired by [Lin et al. \[2024\]](#), which modifies the parameter heuristically to stabilize performance when the line-search regime stalls. Further details on the adaptive scheme are provided in [Section B](#).

3.3 Convergence Guarantee

We now focus on the convergence guarantees of our hybrid algorithm. For ease of reference, we denote $\text{dist}(z, Z^*) := \min_{z^* \in Z^*} \|z - z^*\|$.

The SSN steps of our hybrid algorithm are applied to the residual operator $R_{\text{DRS}}^\gamma(\cdot)$, which enjoys several structural properties that enable a local superlinear convergence guarantee. In particular, by [Lemma 1](#), $R_{\text{DRS}}^\gamma(\cdot)$ is both monotone and Lipschitz continuous, so every choice $G \in \partial R_{\text{DRS}}^\gamma(z)$ in an SSN step will yield a positive semidefinite matrix [[Xiao et al., 2018](#), Lemma 3.5]. Then, the below stability condition is immediately satisfied [[Zhou and Toh, 2005](#), Lemma 3.1].

Lemma 3. *For $G \in \partial R_{\text{DRS}}^\gamma(z)$ and any $\mu > 0$, $\|(G + \mu I)^{-1}\| \leq \frac{1}{\mu}$.*

Moreover, $R_{\text{DRS}}^\gamma(\cdot)$ is piecewise affine. Consequently, it satisfies both strong semi-smoothness ([Lemma 2](#)) and a local error-bound condition described in [Lemma 4](#).

Lemma 4. *For any z in a local neighborhood around a point in Z^* ,*

$$\|R_{\text{DRS}}^\gamma(z)\| \geq \tau \text{dist}(z, Z^*)$$

for some $\tau > 0$.

This local error-bound condition is also known as local metric subregularity. In the context of matrix games, both the duality gap operator [[Gilpin et al., 2012](#)] and the gradient operator $F(z)$ [[Wei et al., 2021](#)] have been shown to satisfy variants of this property. In our setting, the residual operator is piecewise affine and thus polyhedral, which by [Robinson \[1981\]](#) implies local metric subregularity. Thus, we establish a direct extension of prior results and show that the analysis applies more generally to any polyhedral mapping.

These conditions help enforce the local quadratic convergence of the Newton steps of our hybrid algorithm.

Theorem 4. *The regularized semi-smooth Newton method defined by the update rule in [Equation \(2.4\)](#) applied to $R_{\text{DRS}}^\gamma(\cdot)$ exhibits local quadratic convergence. Concretely, there exists a $k_0 \in \mathbb{N}$ such that the iterates $\{z_k\}_{k \geq k_0}$ satisfy*

$$\|R_{\text{DRS}}^\gamma(z_{k+1})\| \leq C \|R_{\text{DRS}}^\gamma(z_k)\|^2 \tag{3.3}$$

where $C = \frac{1}{\tau^2} \left[L_2 \left(2 + \frac{L_2}{\theta\tau} \right)^2 + \theta L_1 \left(2 + \frac{L_2}{\theta\tau} \right) \right]$.

Remark 4. Note that the above result does not rely on θ being fixed (see [Section A.2](#)). Consequently, the final bound in [Equation \(3.3\)](#) also holds in the case where each $\theta_k \in [\underline{\theta}, \bar{\theta}]$, i.e. bounded between fixed lower and upper bounds for θ . This holds in many adaptive methods [[Xiao et al., 2018](#), [Lin et al., 2024](#)], and ours, which vary θ at each time step.

While the above analysis establishes the local quadratic convergence of our residual operator, the analysis applies more generally to any operator satisfying the stated conditions. Our analysis builds on the framework of [Zhou and Toh \[2005\]](#) and extends classical SSN theory by replacing the restrictive BD-regularity assumption [[Xiao et al., 2018](#)] with weaker and more broadly applicable conditions. We outline these conditions in detail below, which must be satisfied for any $z_1, z_2 \in \text{dom}(F)$.

Condition 1. F is L_1 -Lipschitz: for a constant $L_1 > 0$,

$$\|F(z_1) - F(z_2)\| \leq L_1 \|z_1 - z_2\|.$$

Condition 2. F is strongly semi-smooth: for a constant $L_2 > 0$,

$$\|F(z_1) - F(z_2) - G(z_1 - z_2)\| \leq L_2 \|z_1 - z_2\|^2$$

for $G \in \partial F(z_1)$.

Condition 3. F satisfies a local error-bound condition:

$$\|F(z)\| \geq \tau \text{dist}(z, Z^*)$$

for all $z \in N(Z^*)$, where $\tau > 0$.

Condition 4. For $G \in \partial F(z)$ and any $\mu > 0$, $\|(G + \mu I)^{-1}\| \leq \frac{1}{\mu}$.

Remark 5. By our above analysis, if F is monotone and Lipschitz continuous, [Condition 4](#) is immediately satisfied.

In summary, our convergence analysis establishes that the Newton steps of our hybrid algorithm, defined by [Equation \(2.4\)](#), achieves local quadratic convergence when applied to the residual operator $R_{\text{DRS}}^\gamma(\cdot)$. Thus, our hybrid method effectively inherits the best-of-both worlds: global progress from FOMs and rapid local convergence of the regularized SSN method.

4 Numerical Results

We conduct numerical experiments on a variety of matrix games, including Kuhn poker [[Kuhn, 1950](#)], three families of matrix games arising from layered graph security settings [[Černý et al., 2024](#)], and random normal and uniform matrix games. In the realistic game instances, such as Kuhn poker and layered security games, PRM^+ rapidly achieves high-precision last-iterate convergence, making them less suitable for evaluating the benefits of our hybrid SSN algorithm. Accordingly, in this section, we focus on random normal and uniform matrix games, where PRM^+ struggles to efficiently converge to high-precision Nash equilibria.

Our hybrid algorithm is evaluated under two main schemes: **PSSN v1** and **PSSN v2**. These schemes perform a one-time switch from PRM^+ (QA) to the regularized semi-smooth Newton method once the duality gap of the PRM^+ iterates drops under a fixed threshold, but differ in their updating of the damping parameter; the SSN stage of PSSN v1 is initialized with a fixed damping parameter, whereas the SSN stage of PSSN v2 uses a damping parameter tuned by the PRM^+ steps. For completeness, we also include a third scheme, **HPSSN**, in the tables below. HPSSN follows a similar warm-starting strategy but alternates back and forth between PRM^+ and SSN at different rates based on the duality gap, in an effort to reduce the number of costly DRSSN steps while still exploiting curvature information near equilibrium. Although this adaptive alternation is conceptually appealing, in practice it is difficult to tune effectively: varying switching thresholds and the number of DRSSN steps does not consistently yield strong results without extensive tuning.

Our algorithms are compared to PRM^+ last-iterate (LI) and quadratic averaging (QA) baselines, which each use alternation, and are run for 5×10^5 iterations. All algorithms are initialized at $(x, y) = ((1/n)\mathbf{1}_n, (1/m)\mathbf{1}_m)$.

For succinctness, we report numerical results averaged over 10 independently generated random uniform and normal matrix games, of size 400×800 . These games are representative of the general trends we observe across different random matrix game sizes and highlight the efficacy of our hybrid approach over FOMs for achieving high-precision solutions. In particular, despite the one-time cost of calculating resolvents to initialize our DRSSN method, our PSSN algorithms achieve significant speedups in the high-accuracy regime (10^{-8} duality gap or lower), underscoring the practical benefit of incorporating curvature information. Note that, once DRSSN reaches a precision of around 10^{-8} , it takes almost no additional time to reach higher levels of precision, e.g. 10^{-12} . Thus, our numerical experiments corroborate the theoretical superlinear convergence guarantee of our methods.

All other numerical experiments, along with detailed descriptions of the algorithms and game instances, are provided in the appendix.

Table 1: Averaged clock times (in seconds) for 400×800 random uniform matrix games

Method	Time to Reach Duality Gap Tolerance					
	10^{-2}	10^{-4}	10^{-6}	10^{-8}	10^{-10}	10^{-12}
PRM^+ (LI)	0.007	0.059	3.848	21.69		
PRM^+ (QA)	0.006	0.030	0.293	6.424	21.97	
PSSN v1	0.089	0.376	3.463	5.767	5.922	5.940
PSSN v2	0.090	0.385	3.638	4.290	4.307	4.323
HPSSN	0.101	0.399	3.905	5.068	5.082	5.092

Table 2: Averaged clock times (in seconds) for 400×800 random normal matrix games

Method	Time to Reach Duality Gap Tolerance					
	10^{-2}	10^{-4}	10^{-6}	10^{-8}	10^{-10}	10^{-12}
PRM ⁺ (LI)	0.006	0.087	3.325	23.51		
PRM ⁺ (QA)	0.006	0.036	0.366	4.923	19.83	
PSSN v1	0.128	0.690	4.238	5.267	5.289	5.306
PSSN v2	0.128	0.691	3.983	5.055	5.077	5.094
HPSSN	0.125	0.572	3.895	4.786	4.790	4.815

References

- Azam Asl, Haihao Lu, and Jingwen Yang. A J-symmetric quasi-Newton method for minimax problems. *Mathematical Programming*, 204(1):207–254, 2024.
- Heinz H. Bauschke and Patrick L. Combettes. *Convex Analysis and Monotone Operator Theory in Hilbert Spaces*. Springer, 2017.
- Michael Bowling, Neil Burch, Michael Johanson, and Oskari Tammelin. Heads-up limit hold'em poker is solved. *Science*, 347(6218):145–149, 2015.
- Noam Brown and Tuomas Sandholm. Superhuman AI for heads-up no-limit poker: Libratus beats top professionals. *Science*, 359(6374):418–424, 2018.
- Noam Brown and Tuomas Sandholm. Superhuman AI for multiplayer poker. *Science*, 365(6456):885–890, 2019.
- Jakub Černý, Chun Kai Ling, Christian Kroer, and Garud Iyengar. Layered graph security games. In *IJCAI*, pages 2695–2703, 2024.
- Frank H. Clarke. *Optimization and Nonsmooth Analysis*. SIAM, 1990.
- Jonathan Eckstein and Dimitri P. Bertsekas. On the Douglas-Rachford splitting method and the proximal point algorithm for maximal monotone operators. *Mathematical Programming*, 55(1):293–318, 1992.
- Francisco Facchinei and Jong-Shi Pang. *Finite-dimensional Variational Inequalities and Complementarity Problems*. Springer, 2003.
- Meta Fundamental AI Research Diplomacy Team FAIR, Anton Bakhtin, Noam Brown, Emily Dinan, Gabriele Farina, Colin Flaherty, Daniel Fried, Andrew Goff, Jonathan Gray, Hengyuan Hu, et al. Human-level play in the game of diplomacy by combining language models with strategic reasoning. *Science*, 378(6624):1067–1074, 2022.
- Gabriele Farina, Christian Kroer, and Tuomas Sandholm. Faster game solving via predictive blackwell approachability: Connecting regret matching and mirror descent. In *Proceedings of the AAAI Conference on Artificial Intelligence*, volume 35, pages 5363–5371, 2021.

- Andrew Gilpin, Javier Peña, and Tuomas Sandholm. First-order algorithm with $o(\ln(1/\epsilon))$ convergence for ϵ -equilibrium in two-person zero-sum games. *Mathematical Programming*, 133(1-2): 279–298, 2012.
- Galina M. Korpelevich. The extragradient method for finding saddle points and other problems. *Matecon*, 12:747–756, 1976.
- Harold W. Kuhn. Simplified two-person poker. *Contributions to the Theory of Games*, pages 97–103, 1950.
- Bernd Kummer. Newton’s method for non-differentiable functions. *Advances in Mathematical Optimization*, 45(1988):114–125, 1988.
- Tianyi Lin, Marco Cuturi, and Michael I. Jordan. A specialized semismooth Newton method for kernel-based optimal transport. In *AISTATS*, pages 145–153. PMLR, 2024.
- P. L. Lions and B. Mercier. Splitting algorithms for the sum of two nonlinear operators. *SIAM Journal on Numerical Analysis*, 16(6):964–979, 1979.
- José Mario Martínez and Liqun Qi. Inexact Newton methods for solving nonsmooth equations. *Journal of Computational and Applied Mathematics*, 60(1-2):127–145, 1995.
- Robert Mifflin. Semismooth and semiconvex functions in constrained optimization. *SIAM Journal on Control and Optimization*, 15(6):959–972, 1977.
- Arkadi Nemirovski. Prox-method with rate of convergence $o(1/t)$ for variational inequalities with Lipschitz continuous monotone operators and smooth convex-concave saddle point problems. *SIAM Journal on Optimization*, 15(1):229–251, 2004.
- Francesco Orabona. A modern introduction to online learning. *ArXiv Preprint: 1912.13213*, 2019.
- Jong-Shi Pang and Liqun Qi. Nonsmooth equations: Motivation and algorithms. *SIAM Journal on Optimization*, 3(3):443–465, 1993.
- Julien Perolat, Bart De Vylder, Daniel Hennes, Eugene Tarassov, Florian Strub, Vincent de Boer, Paul Muller, Jerome T Connor, Neil Burch, Thomas Anthony, et al. Mastering the game of Stratego with model-free multiagent reinforcement learning. *Science*, 378(6623):990–996, 2022.
- Liqun Qi and Jie Sun. A nonsmooth version of Newton’s method. *Mathematical programming*, 58(1):353–367, 1993.
- Stephen M. Robinson. Some continuity properties of polyhedral multifunctions. In *Mathematical Programming at Oberwolfach*, pages 206–214. 1981.
- R. Tyrrell Rockafellar and Roger J.B. Wets. *Variational Analysis*. Springer, 1998.
- Ernest K. Ryu and Wotao Yin. *Large-scale Convex Optimization: Algorithms & Analyses via Monotone Operators*. Cambridge University Press, 2022.
- Oskari Tammelin. Solving large imperfect information games using CFR+. *ArXiv Preprint: 1407.5042*, 2014.

- Paul Tseng. On linear convergence of iterative methods for the variational inequality problem. *Journal of Computational and Applied Mathematics*, 60(1-2):237–252, 1995.
- Bernhard Von Stengel. Efficient computation of behavior strategies. *Games and Economic Behavior*, 14(2):220–246, 1996.
- Chen-Yu Wei, Chung-Wei Lee, Mengxiao Zhang, and Haipeng Luo. Linear last-iterate convergence in constrained saddle-point optimization. In *ICLR*, 2021.
- Xiantao Xiao, Yongfeng Li, Zaiwen Wen, and Liwei Zhang. A regularized semi-smooth Newton method with projection steps for composite convex programs. *Journal of Scientific Computing*, 76(1):364–389, 2018.
- G. Zhou and K. C. Toh. Superlinear convergence of a Newton-type algorithm for monotone equations. *Journal of Optimization Theory and Applications*, 125(1):205–221, 2005.
- Martin Zinkevich, Michael Johanson, Michael Bowling, and Carmelo Piccione. Regret minimization in games with incomplete information. In *NIPS*, pages 1729–1736, 2007.

A Proofs

A.1 Proofs for Section 2

Recall that the DRS operator is given by

$$T_{\text{DRS}}^\gamma = \text{Id} - J_{N_S}^\gamma + J_F^\gamma \circ (2J_{N_S}^\gamma - \text{Id}),$$

and the residual operator is given by $R_{\text{DRS}}^\gamma = \text{Id} - T_{\text{DRS}}^\gamma$.

Because $F(\cdot)$ is linear and $N_S(\cdot)$ is a normal cone operator, their resolvents simplify to

$$J_F^\gamma(z) = \begin{bmatrix} I & \gamma A \\ -\gamma A^\top & I \end{bmatrix}^{-1} z, \quad J_{N_S}^\gamma(z) = \Pi_S(z).$$

As a consequence, the DRS operator takes the form

$$T_{\text{DRS}}^\gamma = \text{Id} - \Pi_S + \begin{bmatrix} I & \gamma A \\ -\gamma A^\top & I \end{bmatrix}^{-1} (2\Pi_S - \text{Id}).$$

Proof of Lemma 1. For any z_1, z_2 , we have

$$\begin{aligned} & \|R_{\text{DRS}}^\gamma(z_1) - R_{\text{DRS}}^\gamma(z_2)\|^2 \\ &= \|(z_1 - z_2) - (T_{\text{DRS}}^\gamma(z_1) - T_{\text{DRS}}^\gamma(z_2))\|^2 \\ &= \|z_1 - z_2\|^2 + \|T_{\text{DRS}}^\gamma(z_1) - T_{\text{DRS}}^\gamma(z_2)\|^2 - 2(z_1 - z_2)^\top (T_{\text{DRS}}^\gamma(z_1) - T_{\text{DRS}}^\gamma(z_2)). \end{aligned}$$

It is known that T_{DRS}^γ is firmly nonexpansive [Ryu and Yin, 2022]. Equivalently,

$$\|T_{\text{DRS}}^\gamma(z_1) - T_{\text{DRS}}^\gamma(z_2)\|^2 \leq (z_1 - z_2)^\top (T_{\text{DRS}}^\gamma(z_1) - T_{\text{DRS}}^\gamma(z_2)).$$

Putting these pieces together yields

$$\begin{aligned} \|R_{\text{DRS}}^\gamma(z_1) - R_{\text{DRS}}^\gamma(z_2)\|^2 &\leq \|z_1 - z_2\|^2 - (z_1 - z_2)^\top (T_{\text{DRS}}^\gamma(z_1) - T_{\text{DRS}}^\gamma(z_2)) \\ &= (z_1 - z_2)^\top (R_{\text{DRS}}^\gamma(z_1) - R_{\text{DRS}}^\gamma(z_2)). \end{aligned}$$

This implies that $R_{\text{DRS}}^\gamma(\cdot)$ is monotone.

We also have

$$(z_1 - z_2)^\top (R_{\text{DRS}}^\gamma(z_1) - R_{\text{DRS}}^\gamma(z_2)) \leq \|z_1 - z_2\| \|R_{\text{DRS}}^\gamma(z_1) - R_{\text{DRS}}^\gamma(z_2)\|.$$

Thus, we have

$$\|R_{\text{DRS}}^\gamma(z_1) - R_{\text{DRS}}^\gamma(z_2)\| \leq \|z_1 - z_2\|.$$

This implies that $R_{\text{DRS}}^\gamma(\cdot)$ is 1-Lipschitz. \square

Proof of Lemma 2. The strong semi-smoothness of $R_{\text{DRS}}^\gamma(\cdot)$ follows from the existing results that establish the semi-smoothness of projection operators. Since the Euclidean projection onto the product of two simplices is a piecewise affine mapping (polyhedral projection), it is strongly semi-smooth [Qi and Sun, 1993]. See also Facchinei and Pang [2003, Vol. II, Chapter 7] and Robinson [1981]. As such, we have that $\Pi_S(\cdot)$ is strongly semi-smooth. Since the strong semi-smoothness property is closed under scalar multiplication, summation, and composition, the residual map R_{DRS}^γ is strongly semi-smooth. \square

A.2 Proofs for Section 3

Lemma 5 (Equivalence between Projection and Normal Cone). *Let \mathcal{C} be a closed and convex set. Then $p \in \mathcal{C}$ is the projection of x onto \mathcal{C} if and only if $x - p \in N_{\mathcal{C}}(p)$.*

Proof. It is well-known that $p \in \mathcal{C}$ is the projection of x onto \mathcal{C} if and only if

$$\langle y - p, x - p \rangle \leq 0$$

for all $y \in \mathcal{C}$. By the definition of the normal cone, this is equivalent to the condition that $x - p \in N_{\mathcal{C}}(p)$. \square

Proof of Theorem 1 (i). From Equation (2.2), a fixed point z of T_{DRS}^{γ} satisfies

$$z = z - \Pi_{\mathcal{S}}(z) + (I + \gamma F)^{-1}(2\Pi_{\mathcal{S}}(z) - z)$$

or equivalently, $(I + \gamma F)^{-1}(2\Pi_{\mathcal{S}}(z) - z) = \Pi_{\mathcal{S}}(z)$. It follows that

$$(I + \gamma F)(\Pi_{\mathcal{S}}(z)) = 2\Pi_{\mathcal{S}}(z) - z.$$

Expanding and simplifying, we get that $\Pi_{\mathcal{S}}(z) + \gamma F(\Pi_{\mathcal{S}}(z)) = 2\Pi_{\mathcal{S}}(z) - z$, or equivalently,

$$\frac{1}{\gamma}(\Pi_{\mathcal{S}}(z) - z) = F(\Pi_{\mathcal{S}}(z)). \quad (\text{A.1})$$

Furthermore, note that by the first-order optimality condition for projections, we have

$$\frac{1}{\gamma}\langle z - \Pi_{\mathcal{S}}(z), \tilde{z} - \Pi_{\mathcal{S}}(z) \rangle \leq 0$$

for all $\tilde{z} \in \mathcal{S}$, or equivalently,

$$\frac{1}{\gamma}(z - \Pi_{\mathcal{S}}(z)) \in N_{\mathcal{S}}(\Pi_{\mathcal{S}}(z)). \quad (\text{A.2})$$

Summing Equation (A.1) and Equation (A.2), we get the desired result,

$$0 \in F(\Pi_{\mathcal{S}}(z)) + N_{\mathcal{S}}(\Pi_{\mathcal{S}}(z)).$$

By the optimality condition for a Nash equilibrium, $\hat{z} = \Pi_{\mathcal{S}}(z)$ is a Nash equilibrium. \square

Proof of Theorem 1 (ii). Since \hat{z} is a Nash equilibrium, we have that $0 \in F(\hat{z}) + N_{\mathcal{S}}(\hat{z})$. Equivalently, $u := -F(\hat{z}) \in N_{\mathcal{S}}(\hat{z})$.

Consider $z := \hat{z} - \gamma F(\hat{z}) = \hat{z} + \gamma u$. Since $\hat{z} \in \mathcal{S}$ and $u \in N_{\mathcal{S}}(\hat{z})$ implies that $(\hat{z} + \gamma u) - \hat{z} = \gamma u \in N_{\mathcal{S}}(\hat{z})$, by Lemma 5, we have that $\hat{z} = \Pi_{\mathcal{S}}(\hat{z} + \gamma u)$. It follows that $\Pi_{\mathcal{S}}(z) = \Pi_{\mathcal{S}}(\hat{z} + \gamma u) = \hat{z}$, and we have that

$$\begin{aligned} 2\Pi_{\mathcal{S}}(z) - z &= 2\Pi_{\mathcal{S}}(\hat{z} + \gamma u) - (\hat{z} + \gamma u) \\ &= 2\hat{z} - (\hat{z} + \gamma u) \\ &= \hat{z} - \gamma u. \end{aligned}$$

Applying T_{DRS}^γ to the lifted point z , we get that

$$\begin{aligned}
T_{\text{DRS}}^\gamma(z) &= z - \Pi_{\mathcal{S}}(z) + (I + \gamma F)^{-1}(2\Pi_{\mathcal{S}}(z) - z) \\
&= (\hat{z} + \gamma u) - \hat{z} + (I + \gamma F)^{-1}(\hat{z} - \gamma u) \\
&= (\hat{z} + \gamma u) - \hat{z} + (I + \gamma F)^{-1}(\hat{z} + \gamma F(\hat{z})) \\
&= (\hat{z} + \gamma u) - \hat{z} + \hat{z} \\
&= \hat{z} + \gamma u = z
\end{aligned}$$

where the third line follows from the definition $u = -F(\hat{z})$. Thus, $z = \hat{z} - \gamma F(\hat{z})$ is a fixed point of T_{DRS}^γ . \square

Proof of Theorem 2. For any $i \in \mathcal{A}$, the closed-form simplex projection formula gives

$$x_i = p_i - \alpha, \text{ where } \alpha = \frac{1}{|\mathcal{A}|} \left(\sum_{j \in \mathcal{A}} p_j - 1 \right)$$

For $i \notin \mathcal{A}$, we have $x_i = 0$. Differentiating with respect to p_j , we get, for $i \in \mathcal{A}$,

$$G_{ij} = \frac{\partial x_i}{\partial p_j} = \begin{cases} 1 - \frac{1}{|\mathcal{A}|}, & \text{if } i = j \in \mathcal{A} \\ -\frac{1}{|\mathcal{A}|} & \text{if } j \in \mathcal{A}, i \neq j \\ 0 & \text{if } j \notin \mathcal{A} \end{cases}$$

On the other hand, for $i \notin \mathcal{A}$, we trivially have $G_{ij} = 0$ for all j . Equivalently, the Jacobian admits the compact representation

$$G = \text{diag}(a) - \frac{1}{\|a\|_1} a a^\top$$

where a is the indicator vector of the active set \mathcal{A} . \square

Lemma 6. For any two points $z_1 = (x_1 y_1) \in \mathcal{S}$ and $z_2 = (x_2 y_2) \in \mathcal{S}$, we have

$$|\text{gap}(z_1) - \text{gap}(z_2)| \leq \sqrt{2} \|A\| \cdot \|z_1 - z_2\|.$$

Proof of Lemma 6. By definition,

$$\text{gap}(x, y) = \max_{\bar{y} \in Y} x^\top A \bar{y} - \min_{\bar{x} \in X} \bar{x}^\top A y.$$

Let us define $\Phi(x) := \max_{\bar{y} \in Y} x^\top A \bar{y}$ and $\Psi(y) := \min_{\bar{x} \in X} \bar{x}^\top A y$, so that $\text{gap}(x, y) = \Phi(x) - \Psi(y)$.

We have that

$$\begin{aligned}
\Phi(x_1) - \Phi(x_2) &= \max_{\bar{y} \in Y} x_1^\top A \bar{y} - \max_{\hat{y} \in Y} x_2^\top A \hat{y} \\
&\leq \max_{\bar{y} \in Y} [x_1^\top A \bar{y} - x_2^\top A \bar{y}] \\
&= \max_{\bar{y} \in Y} \langle x_1 - x_2, A \bar{y} \rangle \\
&\leq \|A\| \cdot \|x_1 - x_2\|.
\end{aligned}$$

where the last line follows by the Cauchy-Schwarz inequality and the fact that $\|y\| \leq 1$ for all $y \in \Delta^n$. The above result also implies that

$$\Phi(x_2) - \Phi(x_1) \leq \|A\| \cdot \|x_2 - x_1\|.$$

Combining the above two results, we get that

$$|\Phi(x_1) - \Phi(x_2)| \leq \|A\| \cdot \|x_1 - x_2\|. \quad (\text{A.3})$$

Similarly, we have that

$$\begin{aligned} \Psi(y_1) - \Psi(y_2) &= \min_{\bar{x} \in X} \bar{x}^\top A y_1 - \min_{\hat{x} \in X} \hat{x}^\top A y_2 \\ &\leq \max_{\bar{x} \in X} [\bar{x}^\top A y_1 - \bar{x}^\top A y_2] \\ &= \max_{\bar{x} \in X} \langle \bar{x}, A(y_1 - y_2) \rangle \\ &\leq \|A\| \cdot \|y_1 - y_2\| \end{aligned}$$

where the last line follows by the Cauchy-Schwarz inequality and the fact that $\|x\| \leq 1$ for all $x \in \Delta^m$. The above result also implies that

$$\Psi(y_2) - \Psi(y_1) \leq \|A\| \cdot \|y_2 - y_1\|.$$

Combining the above two results, we get that

$$|\Psi(y_1) - \Psi(y_2)| \leq \|A\| \cdot \|y_1 - y_2\|. \quad (\text{A.4})$$

Since

$$\begin{aligned} \text{gap}(z_1) - \text{gap}(z_2) &= \text{gap}(x_1, y_1) - \text{gap}(x_2, y_2) \\ &= (\Phi(x_1) - \Psi(y_1)) - (\Phi(x_2) - \Psi(y_2)) \\ &= (\Phi(x_1) - \Phi(x_2)) - (\Psi(y_1) - \Psi(y_2)), \end{aligned}$$

we have that

$$\begin{aligned} |\text{gap}(z_1) - \text{gap}(z_2)| &= |\Phi(x_1) - \Phi(x_2) + \Psi(y_1) - \Psi(y_2)| \\ &\leq |\Phi(x_1) - \Phi(x_2)| + |\Psi(y_1) - \Psi(y_2)| \\ &\leq \|A\| \cdot (\|x_1 - x_2\| + \|y_1 - y_2\|) \\ &\leq \sqrt{2} \|A\| \cdot \|z_1 - z_2\| \end{aligned}$$

where the third line follows from applying the bounds of [Equation \(A.3\)](#) and [Equation \(A.4\)](#) and the final line follows from an application of the inequality $a + b \leq \sqrt{2}\sqrt{a^2 + b^2}$ where $a = \|x_1 - x_2\|$, $b = \|y_1 - y_2\|$, and so $\sqrt{a^2 + b^2} = \|z_1 - z_2\|$. \square

Proof of [Theorem 3](#) (i). Let z^* be the closest optimal solution to z in Z^* . Rewriting the given condition $\|R_{\text{DRS}}^\gamma(z)\| \geq \tau \|z - z^*\|$, we have

$$\|z - z^*\| \leq \frac{\|R_{\text{DRS}}^\gamma(z)\|}{\tau}. \quad (\text{A.5})$$

Let us define $\hat{z} := \Pi_{\mathcal{S}}(z)$ and $\hat{z}^* := \Pi_{\mathcal{S}}(z^*)$. Since projection is a nonexpansive operator, we have that

$$\|\hat{z} - \hat{z}^*\| \leq \|z - z^*\|. \quad (\text{A.6})$$

Furthermore, by [Lemma 6](#) applied to \hat{z} and \hat{z}^* , we have that

$$|\text{gap}(\hat{z}) - \text{gap}(\hat{z}^*)| \leq \sqrt{2}\|A\| \cdot \|\hat{z} - \hat{z}^*\| \quad (\text{A.7})$$

Combining the results of [Equation \(A.5\)](#), [Equation \(A.6\)](#), and [Equation \(A.7\)](#), we get that

$$|\text{gap}(\hat{z}) - \text{gap}(\hat{z}^*)| \leq \sqrt{2}\|A\| \cdot \|\hat{z} - \hat{z}^*\| \leq \sqrt{2}\|A\| \cdot \|z - z^*\| \leq \frac{\sqrt{2}\|A\| \cdot \|R_{\text{DRS}}^\gamma(z)\|}{\tau}.$$

By [Theorem 1](#) (i), $\text{gap}(\hat{z}^*) = 0$. Thus, we conclude that

$$|\text{gap}(\hat{z})| = |\text{gap}(\Pi_{\mathcal{S}}(z))| \leq \frac{\sqrt{2}\|A\| \cdot \|R_{\text{DRS}}^\gamma(z)\|}{\tau}. \quad \square$$

Proof of [Theorem 3](#) (ii). Let \hat{z}^* be the closest Nash equilibrium to \hat{z} , so that $\text{dist}(\hat{z}, \hat{Z}^*) = \|\hat{z} - \hat{z}^*\|$. By [Equation \(3.2\)](#), we have that

$$\|\hat{z} - \hat{z}^*\| \leq \frac{\text{gap}(\hat{z})}{\delta(A)}. \quad (\text{A.8})$$

Consider the lifted points $z := \hat{z} - \gamma F(\hat{z})$ and $z^* := \hat{z}^* - \gamma F(\hat{z}^*)$ of \hat{z} and \hat{z}^* , respectively. Note that

$$\begin{aligned} \|z - z^*\| &= \|(\hat{z} - \gamma F(\hat{z})) - (\hat{z}^* - \gamma F(\hat{z}^*))\| \\ &= \|\hat{z} - \hat{z}^* - \gamma(F(\hat{z}) - F(\hat{z}^*))\| \\ &\leq \|\hat{z} - \hat{z}^*\| + \gamma\|A\| \cdot \|\hat{z} - \hat{z}^*\| \\ &= (1 + \gamma\|A\|)\|\hat{z} - \hat{z}^*\| \end{aligned} \quad (\text{A.9})$$

where the third line follows from the triangle inequality and the definition of the operator F .

Finally, by [Lemma 1](#) (ii), we know that $R_{\text{DRS}}^\gamma(\cdot)$ is 1-Lipschitz, so

$$\|R_{\text{DRS}}^\gamma(z)\| = \|R_{\text{DRS}}^\gamma(z) - R_{\text{DRS}}^\gamma(z^*)\| \leq \|z - z^*\|. \quad (\text{A.10})$$

where the first equality follows by [Theorem 1](#) (ii): \hat{z}^* is a Nash equilibrium so its lift z^* satisfies $R_{\text{DRS}}^\gamma(z^*) = 0$.

Thus, we have that

$$\begin{aligned} \|R_{\text{DRS}}^\gamma(z)\| &\leq \|z - z^*\| \\ &\leq (1 + \gamma\|A\|)\|\hat{z} - \hat{z}^*\| \\ &\leq \frac{(1 + \gamma\|A\|)\text{gap}(\hat{z})}{\delta(A)} \end{aligned}$$

where the first line follows from [Equation \(A.10\)](#), the second line follows from [Equation \(A.9\)](#), and the final line follows from [Equation \(A.8\)](#). \square

Proof of Theorem 4. Let z_k^* be the closest optimal solution (zero of R_{DRS}^γ) to z_k . Note that by definition, for $G_k \in R_{\text{DRS}}^\gamma(z_k)$, we have

$$\Delta z_k = -(G_k + \theta \|R_{\text{DRS}}^\gamma(z_k)\| I)^{-1} R_{\text{DRS}}^\gamma(z_k).$$

Adding and subtracting $z_k^* - z_k$ and factoring, we get that

$$\begin{aligned} \Delta z_k &= -(G_k + \theta \|R_{\text{DRS}}^\gamma(z_k)\| I)^{-1} R_{\text{DRS}}^\gamma(z_k) \\ &= -(G_k + \theta \|R_{\text{DRS}}^\gamma(z_k)\| I)^{-1} R_{\text{DRS}}^\gamma(z_k) - (z_k^* - z_k) + (z_k^* - z_k) \\ &= -(G_k + \theta \|R_{\text{DRS}}^\gamma(z_k)\| I)^{-1} [R_{\text{DRS}}^\gamma(z_k) + (G_k + \theta \|R_{\text{DRS}}^\gamma(z_k)\| I)(z_k^* - z_k)] + (z_k^* - z_k). \end{aligned}$$

Taking the norm of both sides, it follows that

$$\|\Delta z_k\| = \left\| -(G_k + \theta \|R_{\text{DRS}}^\gamma(z_k)\| I)^{-1} [R_{\text{DRS}}^\gamma(z_k) + (G_k + \theta \|R_{\text{DRS}}^\gamma(z_k)\| I)(z_k^* - z_k)] + (z_k^* - z_k) \right\|.$$

Applying the Triangle Inequality to the right-hand side and expanding gives

$$\begin{aligned} \|\Delta z_k\| &= \left\| -(G_k + \theta \|R_{\text{DRS}}^\gamma(z_k)\| I)^{-1} [R_{\text{DRS}}^\gamma(z_k) + (G_k + \theta \|R_{\text{DRS}}^\gamma(z_k)\| I)(z_k^* - z_k)] + (z_k^* - z_k) \right\| \\ &\leq \|(G_k + \theta \|R_{\text{DRS}}^\gamma(z_k)\| I)^{-1}\| \cdot \|R_{\text{DRS}}^\gamma(z_k) + G_k(z_k^* - z_k) + \theta \|R_{\text{DRS}}^\gamma(z_k)\| (z_k^* - z_k)\| \\ &\quad + \|z_k^* - z_k\|. \end{aligned}$$

Applying Lemma 3 on the first factor, we get that

$$\begin{aligned} \|\Delta z_k\| &\leq \|(G_k + \theta \|R_{\text{DRS}}^\gamma(z_k)\| I)^{-1}\| \cdot \|R_{\text{DRS}}^\gamma(z_k) + G_k(z_k^* - z_k) + \theta \|R_{\text{DRS}}^\gamma(z_k)\| (z_k^* - z_k)\| \\ &\quad + \|z_k^* - z_k\| \\ &\leq \frac{1}{\theta \|R_{\text{DRS}}^\gamma(z_k)\|} \|R_{\text{DRS}}^\gamma(z_k) + G_k(z_k^* - z_k) + \theta \|R_{\text{DRS}}^\gamma(z_k)\| (z_k^* - z_k)\| + \|z_k^* - z_k\| \\ &\leq \frac{1}{\theta \|R_{\text{DRS}}^\gamma(z_k)\|} (\|R_{\text{DRS}}^\gamma(z_k) - G_k(z_k - z_k^*)\| + \theta \|R_{\text{DRS}}^\gamma(z_k)\| \cdot \|z_k - z_k^*\|) + \|z_k^* - z_k\|. \end{aligned}$$

where the final line follows from the Triangle Inequality. Since $R_{\text{DRS}}^\gamma(\cdot)$ is strongly semi-smooth (Lemma 2), we know that

$$\|R_{\text{DRS}}^\gamma(z_k) - G_k(z_k - z_k^*)\| \leq L_2 \|z_k - z_k^*\|^2$$

for some $L_2 > 0$. Plugging this result in above, we get that

$$\begin{aligned} \|\Delta z_k\| &\leq \frac{1}{\theta \|R_{\text{DRS}}^\gamma(z_k)\|} (\|R_{\text{DRS}}^\gamma(z_k) - G_k(z_k - z_k^*)\| + \theta \|R_{\text{DRS}}^\gamma(z_k)\| \cdot \|z_k - z_k^*\|) + \|z_k^* - z_k\| \\ &\leq \frac{1}{\theta \|R_{\text{DRS}}^\gamma(z_k)\|} (L_2 \|z_k - z_k^*\|^2 + \theta \|R_{\text{DRS}}^\gamma(z_k)\| \cdot \|z_k - z_k^*\|) + \|z_k^* - z_k\| \\ &= 2\|z_k - z_k^*\| + \frac{L_2}{\theta \|R_{\text{DRS}}^\gamma(z_k)\|} \|z_k - z_k^*\|^2. \end{aligned} \tag{A.11}$$

Since $R_{\text{DRS}}^\gamma(\cdot)$ satisfies the local error-bound (Lemma 4), we have that

$$\|R_{\text{DRS}}^\gamma(z_k)\| = \|R_{\text{DRS}}^\gamma(z_k) - R_{\text{DRS}}^\gamma(z_k^*)\| \geq \tau \|z_k - z_k^*\|.$$

Taking the reciprocal of both sides gives

$$\frac{1}{\|R_{\text{DRS}}^\gamma(z_k)\|} \leq \frac{1}{\tau \|z_k - z_k^*\|}.$$

Plugging this bound into the result of [Equation \(A.11\)](#) gives

$$\begin{aligned} \|\Delta z_k\| &\leq 2\|z_k - z_k^*\| + \frac{L_2}{\theta \|R_{\text{DRS}}^\gamma(z_k)\|} \|z_k - z_k^*\|^2 \\ &\leq 2\|z_k - z_k^*\| + \frac{L_2}{\theta \tau \|z_k - z_k^*\|} \|z_k - z_k^*\|^2 \\ &= \left(2 + \frac{L_2}{\theta \tau}\right) \|z_k - z_k^*\|. \end{aligned} \tag{A.12}$$

We now focus on the norm of the residual map at consecutive iterates z_k and z_{k+1} . By definition,

$$\|R_{\text{DRS}}^\gamma(z_{k+1})\| = \|R_{\text{DRS}}^\gamma(z_k + \Delta z_k)\|.$$

Adding and subtracting $R_{\text{DRS}}^\gamma(z_k) + G_k \Delta z_k$ and then applying the Triangle Inequality, we get that

$$\begin{aligned} \|R_{\text{DRS}}^\gamma(z_{k+1})\| &= \|R_{\text{DRS}}^\gamma(z_k + \Delta z_k)\| \\ &= \|R_{\text{DRS}}^\gamma(z_k + \Delta z_k) - R_{\text{DRS}}^\gamma(z_k) - G_k \Delta z_k + R_{\text{DRS}}^\gamma(z_k) + G_k \Delta z_k\| \\ &\leq \|R_{\text{DRS}}^\gamma(z_k + \Delta z_k) - R_{\text{DRS}}^\gamma(z_k) - G_k \Delta z_k\| + \|R_{\text{DRS}}^\gamma(z_k) + G_k \Delta z_k\|. \end{aligned} \tag{A.13}$$

Since $R_{\text{DRS}}^\gamma(\cdot)$ is strongly semi-smooth ([Lemma 2](#)), we once again have that

$$\|R_{\text{DRS}}^\gamma(z_k + \Delta z_k) - R_{\text{DRS}}^\gamma(z_k) - G_k \Delta z_k\| \leq L_2 \|\Delta z_k\|^2. \tag{A.14}$$

On the other hand, by the definition of Δz_k , we have that

$$R_{\text{DRS}}^\gamma(z_k) + (G_k + \theta \|R_{\text{DRS}}^\gamma(z_k)\| I) \Delta z_k = 0.$$

Equivalently, after expanding, rearranging, and taking the norm of both sides, we have that

$$\|R_{\text{DRS}}^\gamma(z_k) + G_k \Delta z_k\| = \theta \|R_{\text{DRS}}^\gamma(z_k)\| \cdot \|\Delta z_k\|. \tag{A.15}$$

Plugging in the results of [Equation \(A.14\)](#) and [Equation \(A.15\)](#) into the final line of [Equation \(A.13\)](#), we get that

$$\begin{aligned} \|R_{\text{DRS}}^\gamma(z_{k+1})\| &\leq \|R_{\text{DRS}}^\gamma(z_k + \Delta z_k) - R_{\text{DRS}}^\gamma(z_k) - G_k \Delta z_k\| + \|R_{\text{DRS}}^\gamma(z_k) + G_k \Delta z_k\| \\ &\leq L_2 \|\Delta z_k\|^2 + \theta \|R_{\text{DRS}}^\gamma(z_k)\| \cdot \|\Delta z_k\|. \end{aligned} \tag{A.16}$$

Substituting the result from [Equation \(A.12\)](#) into the result from [Equation \(A.16\)](#) and factoring, we get that

$$\begin{aligned} \|R_{\text{DRS}}^\gamma(z_{k+1})\| &\leq L_2 \|\Delta z_k\|^2 + \theta \|R_{\text{DRS}}^\gamma(z_k)\| \cdot \|\Delta z_k\| \\ &\leq L_2 \left(2 + \frac{L_2}{\theta \tau}\right)^2 \|z_k - z_k^*\|^2 + \theta \|R_{\text{DRS}}^\gamma(z_k)\| \left(2 + \frac{L_2}{\theta \tau}\right) \|z_k - z_k^*\| \\ &\leq \left[L_2 \left(2 + \frac{L_2}{\theta \tau}\right)^2 + \theta L_1 \left(2 + \frac{L_2}{\theta \tau}\right) \right] \|z_k - z_k^*\|^2 \end{aligned} \tag{A.17}$$

where the final line follows as $R_{\text{DRS}}^\gamma(\cdot)$ is 1-Lipschitz (Lemma 1 (ii)), or equivalently,

$$\|R_{\text{DRS}}^\gamma(z_k)\| = \|R_{\text{DRS}}^\gamma(z_k) - R_{\text{DRS}}^\gamma(z_k^*)\| \leq L_1 \|z_k - z_k^*\|.$$

Since $R_{\text{DRS}}^\gamma(\cdot)$ satisfies the local error-bound condition (Lemma 4), we have that

$$\|R_{\text{DRS}}^\gamma(z_k)\| = \|R_{\text{DRS}}^\gamma(z_k) - R_{\text{DRS}}^\gamma(z_k^*)\| \geq \tau \|z_k - z_k^*\|.$$

Squaring both sides and rearranging, it follows that

$$\|z_k - z_k^*\|^2 \leq \frac{\|R_{\text{DRS}}^\gamma(z_k)\|^2}{\tau^2}$$

Using the above result to bound the right-hand side of Equation (A.17) above, we get that

$$\begin{aligned} \|R_{\text{DRS}}^\gamma(z_{k+1})\| &\leq \left[L_2 \left(2 + \frac{L_2}{\theta\tau} \right)^2 + \theta L_1 \left(2 + \frac{L_2}{\theta\tau} \right) \right] \|z_k - z_k^*\|^2 \\ &\leq \frac{1}{\tau^2} \left[L_2 \left(2 + \frac{L_2}{\theta\tau} \right)^2 + \theta L_1 \left(2 + \frac{L_2}{\theta\tau} \right) \right] \|R_{\text{DRS}}^\gamma(z_k)\|^2. \end{aligned}$$

which gives us the desired local quadratic convergence of Equation (3.3). \square

B Our Algorithm

B.1 Predictive Regret Matching⁺

We first provide an overview of the Predictive Regret Matching⁺ (PRM⁺) algorithm, and then discuss its effectiveness over other first-order methods for game solving.

Description of PRM⁺. At a high level, the classical Regret Matching (RM) algorithm maintains a cumulative regret vector over actions, measuring how much better each pure action would have performed relative to the mixed strategy that is played. At each iteration, the algorithm assigns probability mass only to actions with positive cumulative regret, proportional to the magnitude of that regret. Regret Matching⁺ (RM⁺) is a simple yet powerful modification of this idea; after each update, the cumulative regrets are clipped at zero (using the operator $[\cdot]^+ = \max\{\cdot, 0\}$), thus preventing negative regrets from accumulating and yielding significantly improved empirical performance. The predictive variant PRM⁺ further incorporates a prediction vector m^t directly in its update. This allows the algorithm to estimate the next loss and adjust its iterate in anticipation, rather than reacting only after observing the realized loss ℓ^t . As a result, PRM⁺ exhibits faster convergence in practice.

Below, we provide the pseudocode of PRM⁺, taken directly from Farina et al. [2021].

Algorithm 3 (Predictive) regret matching⁺ [(P)RM⁺]

```
1:  $z^0 \leftarrow 0 \in \mathbb{R}^n, \quad x^0 \leftarrow \frac{1}{n}\mathbf{1} \in \Delta^n$ 
2: function NEXTSTRATEGY( $m^t$ )
3:    $\theta^t \leftarrow [z^{t-1} + \langle m^t, x^{t-1} \rangle \mathbf{1} - m^t]^+$  ▷ Set  $m^t = 0$  for the non-predictive version
4:   if  $\theta^t \neq 0$  then
5:     return  $x^t \leftarrow \theta^t / \|\theta^t\|_1$ 
6:   else
7:     return  $x^t \leftarrow$  arbitrary point in  $\Delta^n$ 
8: function OBSERVELOSS( $\ell^t$ )
9:    $z^t \leftarrow [z^{t-1} + \langle \ell^t, x^t \rangle \mathbf{1} - \ell^t]^+$ 
```

The game solving literature also uses a variety of heuristics for stronger numerical performance. The *quadratic averaging* scheme uses a weighted average of past iterates in which the weight assigned to the iterate at time step t is t^2 , while the *last-iterate* scheme simply uses the last iterate without any averaging. Finally, *alternation* (or *alternating updates*) refers to updating the players sequentially within each iteration, which is commonly used to further improve convergence behavior in practice.

Choice of PRM⁺ as First-Order Method. Our hybrid SSN framework is not tied to PRM⁺ specifically. The theoretical conditions (Theorem 3) governing the transition to the second-order phase depend only on the quality of the current iterate, as measured by the duality gap. Consequently, any first-order method that reliably reduces the duality gap, including those guaranteeing last-iterate (or average) convergence in these zero-sum games, is compatible with our setup.

Our focus on PRM⁺ in our experiments is motivated by the fact that it is the state-of-the-art practical first-order method for large-scale zero-sum games. In particular, the game-solving literature overwhelmingly finds that PRM⁺ and its extensive-form variant PCFR⁺ outperform other first-order methods on saddle-point problems. This is consistent with our own empirical evaluations. For completeness, we report the relative performances of extragradient (EG) and optimistic gradient descent-ascent (OGDA) against PRM⁺ for the 400×800 random matrix games tested in the main body below.

In these experiments, we run both EG and OGDA for 10^5 iterations; this choice is deliberate, as each iteration is more expensive than a PRM⁺ iteration, and the differences in both runtime and performance are already clearly visible.

Across the ten random seeds tested, the symbol (†) indicates that one seed failed to reach the specified duality-gap threshold, while the symbol (*) indicates that nine seeds failed to reach the threshold. EG and OGDA are substantially slower across the full range of tolerances, whereas PRM⁺ reaches comparable accuracy orders of magnitude faster. These results further justify our use of PRM⁺ (with alternation under both quadratic-averaging and last-iterate schemes) as the primary baseline in Table 1 and Table 2.

In summary, the strong empirical performance of PRM⁺, together with its scalability to extensive-form games via PCFR⁺, makes it a natural and representative choice for both benchmarking and warm-starting our hybrid algorithms. We provide further details on the integration of PRM⁺ with our methods in the following sections.

Table 3: Averaged clock times (seconds) for 400×800 random matrix games.
Random Normal

Method	Time to Reach Duality Gap Tolerance					
	10^{-2}	10^{-4}	10^{-5}	$9 \cdot 10^{-6}$	$7.5 \cdot 10^{-6}$	10^{-6}
EG	0.322	7.255	46.532	51.580	59.049	(*)
OGDA	0.070	1.584	10.378	11.381	13.342	(*)
PRM ⁺ (LI)	0.006	0.087	0.465	0.505	0.592	0.851
PRM ⁺ (QA)	0.006	0.036	0.110	0.116	0.131	0.165

Random Uniform

Method	Time to Reach Duality Gap Tolerance				
	10^{-2}	10^{-4}	10^{-5}	$9 \cdot 10^{-6}$	10^{-6}
EG	0.436	9.645	65.302	(†)	(*)
OGDA	0.099	2.140	14.361	16.340	(*)
PRM ⁺ (LI)	0.007	0.059	0.301	0.344	3.848
PRM ⁺ (QA)	0.006	0.030	0.084	0.086	0.293

B.2 Adaptive Scheme

The β_0 coefficient serves as a contraction factor for the damping parameter λ , and its magnitude reflects the relative weight placed on second-order information from $G_k \in \partial R_{\text{DRS}}^\gamma(x_k, y_k)$. As the iterates approach the optimal solution, the residual norm $\|R_{\text{DRS}}^\gamma(x_k, y_k)\|$ decreases, in turn causing β_0 to shrink.

ψ measures the quality of the Newton direction $\begin{bmatrix} \Delta x \\ \Delta y \end{bmatrix}$. A small value of ψ indicates that the direction is not informative, while a large value indicates that the direction is informative and effectively reduces the residual norm. Based on the value of ψ , the adaptive scheme, mirroring that of Lin et al. [2024], for updating λ_{k+1} is as follows:

$$\lambda_{k+1} = \begin{cases} \max\{\underline{\lambda}, \beta_0 \lambda_k\} & \text{if } \psi \geq \alpha_2 \\ \beta_1 \lambda_k & \text{if } \alpha_1 \leq \psi < \alpha_2 \\ \min\{\bar{\lambda}, \beta_2 \lambda_k\} & \text{if } \psi < \alpha_1 \end{cases}$$

Note that this adaptive update rule distinguishes three regimes:

- **High-quality direction** ($\psi \geq \alpha_2$): the step produces significant progress toward an optimal solution, so the damping parameter is moderately decreased by multiplying by a contraction factor $\beta_0 < 1$.
- **Moderate-quality direction** ($\alpha_1 \leq \psi < \alpha_2$): the step produces moderate but not significant progress towards an optimal solution, so the damping parameter is moderately increased by a factor $\beta_1 > 1$.
- **Low-quality direction** ($\psi < \alpha_1$): the step produces little to no progress toward an optimal solution, so the damping parameter is significantly increased by a factor $\beta_2 \gg 1$.

In our experiments, we use the parameters $\alpha_1 = 10^{-2}$, $\alpha_2 = 5$, $\beta_1 = 2$, $\beta_2 = 5$, $\underline{\lambda} = 10^{-15}$, and $\bar{\lambda} = 10^{15}$.

B.3 Description of Hybrid Algorithms

PSSN v1 performs a one-time switch from PRM^+ with quadratic averaging and alternation to the DRSSN method once the duality gap drops under some specified fixed threshold. After switching, the SSN method is initialized with a fixed damping parameter of 1 and is run exclusively thereafter. This makes PSSN v1 the simplest hybrid variant, but its rigidity in fixing the damping parameter can limit its speed across different problem instances.

PSSN v2 also performs a one-time switch from PRM^+ with quadratic averaging and alternation to the DRSSN method once the duality gap drops under some specified fixed threshold. Every 500 PRM^+ iterations, the damping parameter is iteratively updated using the adaptive scheme. After switching, the SSN method is initialized with this updated damping parameter. As a result, PSSN v2 is often more adapted to the dynamics of the problem, and often achieves better stability and efficiency than PSSN v1, although at the cost of some additional updating during the PRM^+ phase.

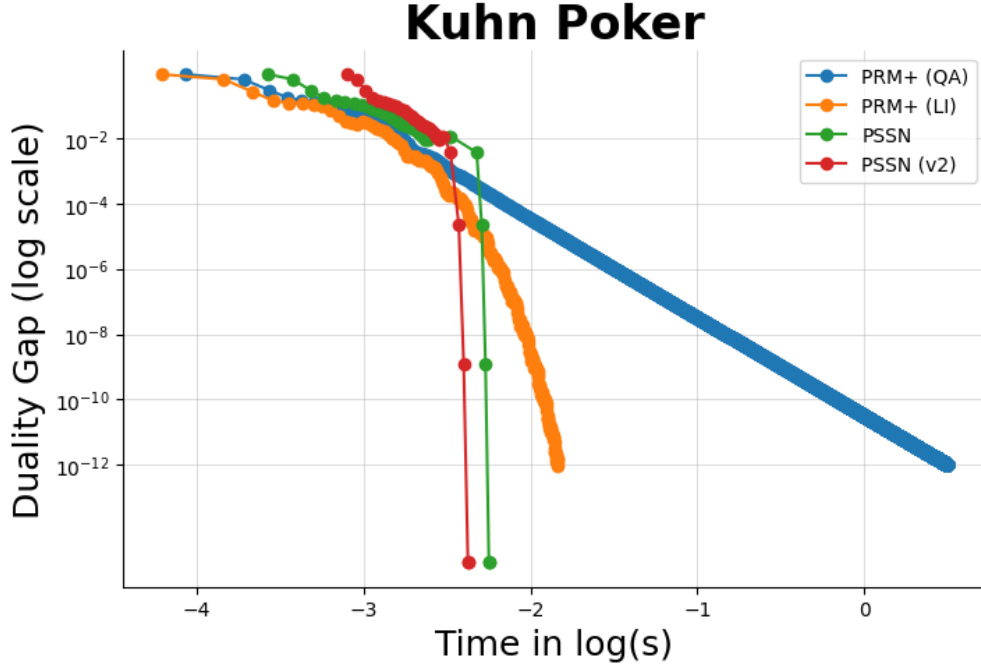
HPSSN adopts a more dynamic approach, alternating between PRM^+ and DRSSN throughout the run. At different stages, the algorithm attempts to lift a PRM^+ iterate and switch into DRSSN, taking only a few Newton steps before deciding whether superlinear convergence is being achieved. If not, it projects the current iterate back onto \mathcal{S} and switches back to PRM^+ . This strategy attempts to reduce the number of system solves from the SSN steps while still exploiting curvature information near equilibrium, striking a balance between the low per-iteration cost of first-order methods and the fast local convergence of second-order methods. We reiterate the discussion of [Section 4](#): though this idea is conceptually appealing, it is difficult to tune effectively in practice and depends heavily on each problem instance. Given these shortcomings, we only include it in the 400×800 matrix game experiments.

C Additional Numerical Experiments

We provide both detailed descriptions for each game instance and additional tests comparing our algorithms to the PRM^+ baselines.

C.1 Realistic Game Instances

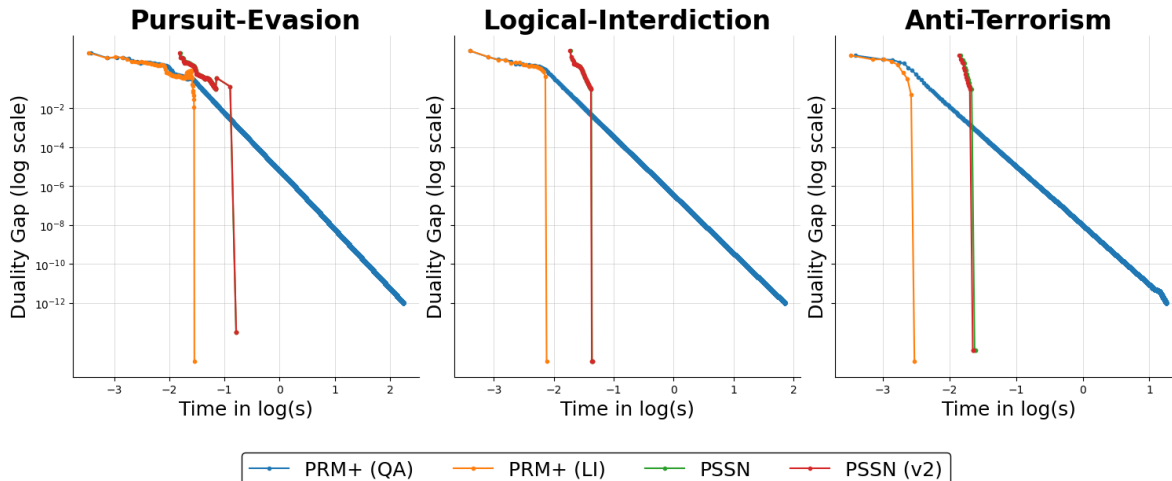
Kuhn poker [[Kuhn, 1950](#)]. At the beginning of the game, the two players each pay one chip to the pot, and are dealt a single private card from a deck containing three cards: Jack, Queen, and King. The first player can check or bet, putting an additional chip in the pot. Then, the second player can check or bet after the first player’s check, or fold/call the first player’s bet. If the second player bets, the first player can decide whether to fold or to call the bet. At the showdown, the player with the highest card who has not folded wins all the chips in the pot. The payoff matrix for Kuhn poker has dimension 27×64 with 690 nonzeros.



Kuhn poker is a standard benchmark in the game-theoretic literature and is widely used as a baseline for evaluating algorithms. However, its small size makes it straightforward to solve exactly. Even so, we observe improvements with our PSSN methods, which switch at a loose threshold of 10^{-2} , over the last-iterate PRM^+ algorithm, and our methods also outperform PRM^+ with quadratic averaging and alternation.

Layered graph security games [Černý et al., 2024]. We test on three classes of layered graph security games: the pursuit-evasion, logical-interdiction, and anti-terrorism games. Detailed descriptions of these instances can be found in Černý et al. [2024].

For all layered graph security game tests, we use the random seed 2025 together with the default parameter settings from the associated GitHub repository. The payoff matrix for the pursuit-evasion game has dimension 119×887 with 70253 nonzeros, the payoff matrix for the logical-interdiction game has dimension 119×856 with 2931 nonzeros, and the payoff matrix for the anti-terrorism game has dimension 119×1080 with 3756 nonzeros.



In these instances, the last-iterate PRM^+ algorithm solves the game directly and our PSSN methods solves the game quickly after switching at a relatively loose threshold of 10^{-1} . We note that these instances clearly do not require the use of curvature information to find an efficient solution. However, our results still outperform PRM^+ with quadratic averaging and alternation, the de-facto approach to game solving. This motivates our focus on random matrix games in our experiments; in random matrix instances, PRM^+ struggles to efficiently converge to a high-precision solution, and we find that our PSSN algorithms can do so extremely effectively.

C.2 Random Game Instances

The following tests are run on 10 independently generated random seeds across two classes of random matrices. In the uniform case, each entry A_{ij} is drawn uniformly from $[-1, 1]$, while in the normal case, each entry A_{ij} is drawn i.i.d from a standard normal distribution. We generate these instances on matrices of size $n \times m$ for $(n, m) = (100, 100), (400, 400)$, and $(400, 800)$.

We first test our methods across different duality gap switching thresholds. The best thresholds, in terms of lowest average clock times, are colored in blue.

Table 4: Averaged clock times (seconds) for 100×100 random matrix games vs thresholds.

<i>Random Uniform</i>					<i>Random Normal</i>				
Method	Duality Gap Switching Threshold				Method	Duality Gap Switching Threshold			
	10^{-1}	10^{-2}	10^{-3}	10^{-4}		10^{-1}	10^{-2}	10^{-3}	10^{-4}
PSSN v1	0.088	0.100	0.113	0.180	PSSN v1	0.118	0.106	0.123	0.182
PSSN v2	0.083	0.098	0.111	0.180	PSSN v2	0.116	0.105	0.120	0.186

Table 5: Averaged clock times (seconds) for 400×400 random matrix games vs thresholds.

<i>Random Uniform</i>					<i>Random Normal</i>				
Method	Duality Gap Switching Threshold				Method	Duality Gap Switching Threshold			
	10^{-4}	10^{-5}	10^{-6}	10^{-7}		10^{-4}	10^{-5}	10^{-6}	10^{-7}
PSSN v1	3.154	2.645	4.213	6.866	PSSN v1	3.762	2.645	4.519	7.132
PSSN v2	2.939	2.424	17.269	23.693	PSSN v2	3.446	3.068	26.445	39.878

Table 6: Averaged clock times (seconds) for 400×800 random matrix games vs thresholds.

<i>Random Uniform</i>					<i>Random Normal</i>				
Method	Duality Gap Switching Threshold				Method	Duality Gap Switching Threshold			
	10^{-4}	10^{-5}	10^{-6}	10^{-7}		10^{-4}	10^{-5}	10^{-6}	10^{-7}
PSSN v1	9.070	5.940	4.648	6.839	PSSN v1	35.320	5.306	33.993	10.827
PSSN v2	9.578	4.323	5.125	74.38	PSSN v2	34.497	5.094	89.87	119.25

Across sizes and distributions, the best switching threshold is not universal and depends heavily on matrix dimension and problem structure. We note that smaller, better-conditioned matrix games (such as the randomly generated 100×100 instances) benefit from earlier or immediate switching, while larger, more ill-conditioned matrix games (such as the randomly generated 400×400 and 400×800 instances) require tighter thresholds for switching to the SSN phase. At the same time, we also note the tradeoff implicit in updates of the damping parameter: updating too aggressively can destabilize the SSN phase, whereas setting the threshold too tightly can delay the switch, causing PRM⁺ to run excessively long before the benefits of second-order acceleration are realized.

Table 7: Averaged clock times (seconds) for 100×100 random matrix games.

<i>Random Normal</i>						
Method	Time to Reach Duality Gap Tolerance					
	10^{-2}	10^{-4}	10^{-6}	10^{-8}	10^{-10}	10^{-12}
PRM ⁺ (LI)	0.008	0.120	4.476	31.205		
PRM ⁺ (QA)	0.008	0.050	0.471	6.238	26.312	
PSSN v1	0.035	0.105	0.116	0.117	0.118	0.118
PSSN v2	0.035	0.102	0.114	0.115	0.115	0.116

<i>Random Uniform</i>						
Method	Time to Reach Duality Gap Tolerance					
	10^{-2}	10^{-4}	10^{-6}	10^{-8}	10^{-10}	10^{-12}
PRM ⁺ (LI)	0.009	0.077	5.170	30.808		
PRM ⁺ (QA)	0.008	0.041	0.396	8.452	27.946	
PSSN v1	0.022	0.070	0.086	0.087	0.088	0.088
PSSN v2	0.020	0.066	0.081	0.082	0.083	0.083

Table 8: Averaged clock times (seconds) for 400×400 random matrix games.

Random Normal

Method	Time to Reach Duality Gap Tolerance					
	10^{-2}	10^{-4}	10^{-6}	10^{-8}	10^{-10}	10^{-12}
PRM ⁺ (LI)	0.005	0.088	3.140	22.092		
PRM ⁺ (QA)	0.005	0.034	0.332	4.258	18.042	
PSSN v1	0.075	0.463	2.608	2.631	2.641	2.645
PSSN v2	0.077	0.481	2.972	3.052	3.064	3.068

Random Uniform

Method	Time to Reach Duality Gap Tolerance					
	10^{-2}	10^{-4}	10^{-6}	10^{-8}	10^{-10}	10^{-12}
PRM ⁺ (LI)	0.006	0.054	3.608	20.130		
PRM ⁺ (QA)	0.005	0.027	0.268	5.755	18.877	
PSSN v1	0.075	0.375	2.538	2.629	2.640	2.645
PSSN v2	0.075	0.375	2.319	2.410	2.417	2.424

In Table 7 and Table 8, we report average clock times across 10 independent random uniform and normal matrix games of sizes 100×100 and 400×400 , respectively. For the smaller 100×100 instances, results are shown with a switching threshold of 10^{-1} , which reflects the fact that such problems are well-conditioned and allow earlier switching into the DRSSN phase without loss of stability. In contrast, the results for the larger, more ill-conditioned 400×400 instances are shown with a tighter switching threshold of 10^{-5} to ensure that the DRSSN method is initialized within a local convergence regime. These thresholds correspond to the optimal switching values identified in Table 4 and Table 5, and are used here to provide an accurate performance comparison. Again, the results across these two tables highlight how the problem size and conditioning affect the choice of switching threshold, and illustrate the robustness of our hybrid method in both moderate and large-scale random matrix settings.

D LLM Usage

The authors used ChatGPT to aid/polish writing.